Journal of Radioanalytical and Nuclear Chemistry (2025) 334:2729–2739
https://doi.org/10.1007/s10967-025-10012-6

Kinetics study of fission products' extraction with attenuated total internal reflection IR spectroscopy

Igor V. Smirnov[1,2] · **Maria D. Karavan**[1,2] · **Timofey S. Aleksandrov**[1,2] · **Alexander A. Brechalov**[1,2] · **Ekaterina S. Babitova**[1,2] · **Vladislav V. Timoshenko**[1] · **Yuri E. Ermolenko**[1]

Received: 12 November 2024 / Accepted: 24 January 2025 / Published online: 10 February 2025

Abstract

A new method for extraction kinetics studying in a biphasic system using time-lapse recording of IR absorption spectra in the attenuated total internal reflection (ATR IR) geometry is developed. The method is examined by studying the extraction process of europium, yttrium and cesium ions with various extractants both from acidic and carbonate media. The mechanism of step-wise coordination with functional groups of the ligand is proposed. The extraction kinetics constants are calculated for the extraction systems with europium. The main advantages of the new method are miniaturization and rapidity, compared to classical methods.

Keywords Extraction · Kinetics · Europium · Cesium · ATR IR spectroscopy

Introduction

Currently, one of the important tasks of the industry is the separation of metals with similar properties, for example, in hydrometallurgy it is necessary to separate metal pairs to obtain individual rare earth elements such as Zr/Hf, Nb/Ta, Ni/Co. Also, the rapid development of the nuclear industry in the world requires close attention to the problems of spent nuclear fuel (SNF) processing and high-level waste (HLW) fractionation. First of all, it is necessary to increase the efficiency and radiation safety of the nuclear industry. In this regard, there is a need for continuous improvement of technologies for the separation and concentration of rare earth element and actinide radionuclides, as well as a number of high-energy isotopes such as cesium-137 and strontium-90.

One of the most common methods for separating and concentrating radionuclides is solvent extraction. Information on the required phase contact time is of great importance in modern radiochemistry, as it allows to reduce the one-time loading of active components and, thereby, significantly reduce the radiation impact on the extractant. The ability of rapid studying the extraction kinetics can allow the selection of effective extractants used in centrifugal extractors, where the phase contact time is extremely short [1, 2]. There are currently many methods used to study extraction kinetics, the most common of them are the single drop technique [3–5], the Lewis diffusion cell method [6–10], microfluidic extraction [11, 12], and the AKUFVE apparatus ("apparatus for continuous measurement of distribution factors in solvent extraction") [13]. The main disadvantages of these methods are the use of large volumes of aqueous and organic phases to be studied, the long duration of the analysis or the complexity of processing the obtained data [11]. In this paper, we propose a new method for studying extraction kinetics using attenuated total reflection infrared spectroscopy (ATR IR). The ATR-IR method is based on the phenomenon of total internal reflection of light, propagating through an optically dense internal reflecting element (crystal). At the interface between the crystal and the sample, an evanescent wave is generated, penetrating the sample to a depth of several nanometers to several microns. This wave interacts with molecules adsorbed on the surface, allowing to study their spectra [14]. ATR IR is a convenient method for studying both solid and liquid samples, when the sample is in direct contact with the ATR crystal attachment. It becomes possible to use small amounts of samples and study various

---

✉ Maria D. Karavan
mkaravan@khlopin.ru

[1] Institute of Chemistry, Saint-Petersburg State University, Universitetskaya Emb., 7 – 9, Saint-Petersburg, Russia 199034

[2] Khlopin Radium Institute, 2nd Murinsky Pr., 28, Saint-Petersburg, Russia 194021

samples without any sample preparation. Due to these properties, the IR ATR method allows to study the kinetics of chemical processes of the widest spectrum [15, 16]. The IR ATR method was developed and examined on various extraction systems (phosphine oxides, crown ethers, heterocyclic phenols) proposed for the fission products extraction from nitric acid and carbonate media. We compared the IR ATR experimental results with those, obtained by the classical method—with a Lewis diffusion cell.

Experimental

Materials and techniques

Extractants (Table 1)—triamylphosphine oxide (TAPO), octyl(phenyl)-N,N-diisobutylcarbamoyl-methylphosphine oxide (CMPO), di-tert-butyldibenzo-18-crown-6 ether (DTBDB18C6), N,N,N’,N’-tetraoctyldiamide diglycolic acid (TODGA), and 8-hydroxyquinoline (8-HQ) were obtained from Khlopin Radium Institute (Russia), organic solvents—dichloroethane (DCE) and tetrachloroethylene (TCE) were purchased from Ekos (Russia), europium and cesium nitrates—$Eu(NO_3)_3 \cdot 6H_2O$ and $CsNO_3$ were produced by Vekton (Russia), yttrium carbonate $Y_2(CO_3)_3 \cdot 5H_2O$ was from Chemcraft (Russia).

The FTIR absorption spectra were measured on a Simex FT-800 spectrometer (Simex, Russia) using a Simex ATR-A attachment (Simex, Russia) with a diamond crystal (operating surface diameter 2.4 mm). The measurements were carried out in the spectral range 500–4000 cm^{-1} with a resolution 2 cm^{-1}. Calorimetric mixing studies were carried out on a Setaram C80 Calvet calorimeter (Setaram, France). A TA Instruments Nano ITC 2G titration microcalorimeter (TA Instruments, USA) was used for calorimetric titration.

Solutions preparation

An aqueous solution of europium with a concentration of 0.6 mol·L^{-1} was prepared by dissolving 6.69 g of $Eu(NO_3)_3 \cdot 6H_2O$ in a 25 mL volumetric flask. To study the kinetics of extraction from nitric acid media, cesium

Table 1 Extraction systems and recovered cations

№	Cation	Extraction system	Structural formula of the extractant
1	Eu^{3+}	triamylphosphine oxide (TAPO) in dichloroethane	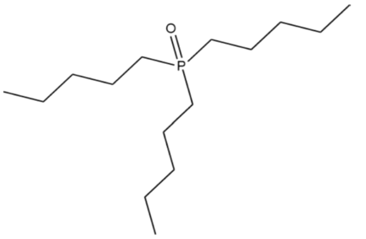
2		octyl(phenyl)-N,N-diisobutylcarbamoyl-methylphosphine oxide (CMPO) in dichloroethane	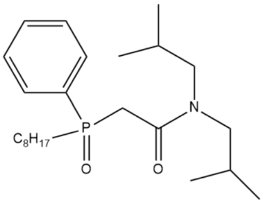
3		N,N,N’,N’-tetraoctyldiamide diglycolic acid (TODGA) in tetrachloroethylene	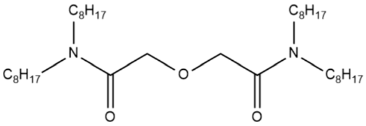
4	Cs^{+}	di-tert-butyldibenzo-18-crown-6 ether (DTBDB18C6) in dichloroethane	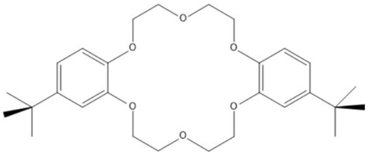
5	Y^{3+}	8-hydroxyquinoline (8-HQ) in dichloroethane	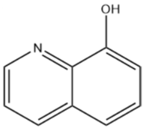

solutions with a cesium concentration of 0.3 mol·L^{-1} and nitric acid concentrations of 1 mol·L^{-1} and 2.5 mol·L^{-1} were prepared. For this purpose, 1.46 g samples of $CsNO_3$ were dissolved in 25 mL volumetric flasks, then 1.79 mL and 4.46 mL of 14 mol·L^{-1} HNO_3 were added to the resulting solutions, respectively. To study the kinetics of extraction from carbonate-alkaline media, an yttrium solution with yttrium concentration of 0.1 mol·L^{-1} and a potassium carbonate concentration of 3 mol·L^{-1} was prepared. In this case, 10.37 g of K_2CO_3 were dissolved in a 25 mL volumetric flask and 0.89 g of $Y_2(CO_3)_3$ were added to the resulting solution. After complete dissolution of the reagents, the resulting solutions were saturated with an organic solvent (DCE or TCE) by adding 0.5 mL of the organic solvent and stirring on a shaker for 10 min. Then the solutions were centrifuged and the aqueous phases were used for experiments. A 0.6 mol·L^{-1} TAPO solution was prepared by dissolving a precise weighed portion of TAPO (3.9 g) in DCE in a 25 mL volumetric flask. The 0.6 mol·L^{-1} solutions of CMPO, DTBD18C6, and 8-HQ were also prepared in 25 mL volumetric flasks by dissolving in DCE. A 0.6 mol·L^{-1} TODGA solution was prepared by dissolving the precise weighed portion in TCE, because the TODGA solution in DCE has a lower density than the $Eu(NO_3)_3$ solution. It is critical for the ATR IR method, since it is necessary for the organic phase to contact the ATR diamond of the attachment. After preparation, all extractant solutions were saturated with water by adding 0.5 mL of distilled water and shaking for 10 min on a shaker. The solutions were then centrifuged and the organic phases were used for the experiments.

Measurement of ATR FTIR spectra

The measurements were performed in the spectral range 500–3500 cm^{-1} with a resolution 2 cm^{-1}. When studying the kinetics of europium extraction in different systems, the spectra were recorded every 3 s, and when studying the extraction rate in the system of cesium and DTBDB18C6—every 10 s. This difference in the recording rates was chosen according to the preliminary experiments, showed that in the system of cesium and DTBDB18C6 the equilibrium is attained in at least 90 min.

The kinetic experiments were carried out in a microcell (Fig. 1), a polypropylene tube ($d = 4.6$ or 8 mm) with a hole in the upper side part for the liquid samples injection.

Samples were injected with a 50 µL chromatographic syringe or with a 100 µL dispenser. During the experiments, the microcell was positioned so that the cell material did not contact with the ATR crystal and was pressed using the ATR press attachment to reduce liquid evaporation. The extractant solution was injected into the cell and the initial spectrum was recorded. Then the aqueous phase was injected into the cell and the spectra recording turned on (one spectrum every 3 or 10 s). The spectra recording continued until no changes were observed at the characteristic wavelengths over 4–5 scans.

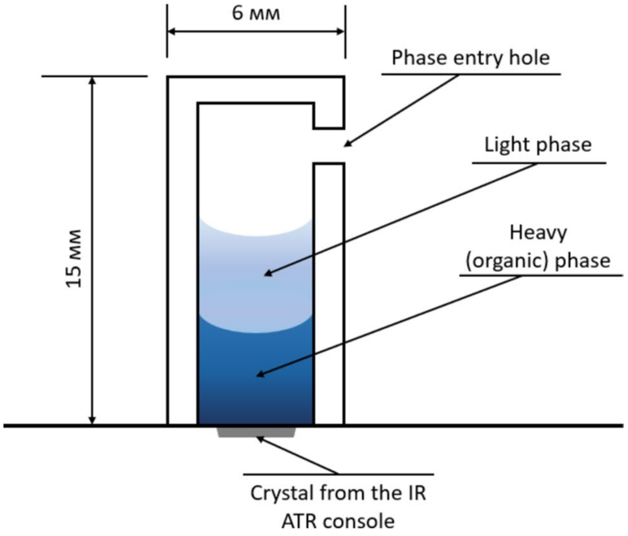

Fig. 1 A microcell for the extraction kinetics studying using the ATR IR method

Extraction kinetics studying by the Lewis diffusion cell method

A Lewis cell was made to study the extraction kinetics by the classical method (Fig. 2). For this purpose, a 50 mL graduated faulcon was cut to a volume of 15 µL. The organic phase was stirred with a magnetic stirrer, and the aqueous phase was stirred with an overhead stirrer. The volume of each phase during the Lewis cell extraction study was 10 µL. Sampling was performed from the aqueous phase using a 100 µL dispenser (the volume of each sample was 50 µL). The samples were diluted 2500 times with 0.1 mol·L^{-1} HNO_3 solution and then analyzed by inductively coupled plasma atomic emission spectroscopy.

Results and discussion

Extraction kinetics in the system of europium and TAPO

The ATR IR spectra in the extraction system of europium (0.6 mol·L^{-1} $Eu(NO_3)_3$) and TAPO (0.6 mol·L^{-1}) in dichloroethane were recorded for 150 s (Fig. 3).

As one can see from the overall IR spectra, the greatest changes occur in the region 2400–2300 cm^{-1} (peaks of carbon dioxide) and the region 1200–1080 cm^{-1} (Fig. 4). This region contains a band of $\nu_{P=O}$ stretching vibrations

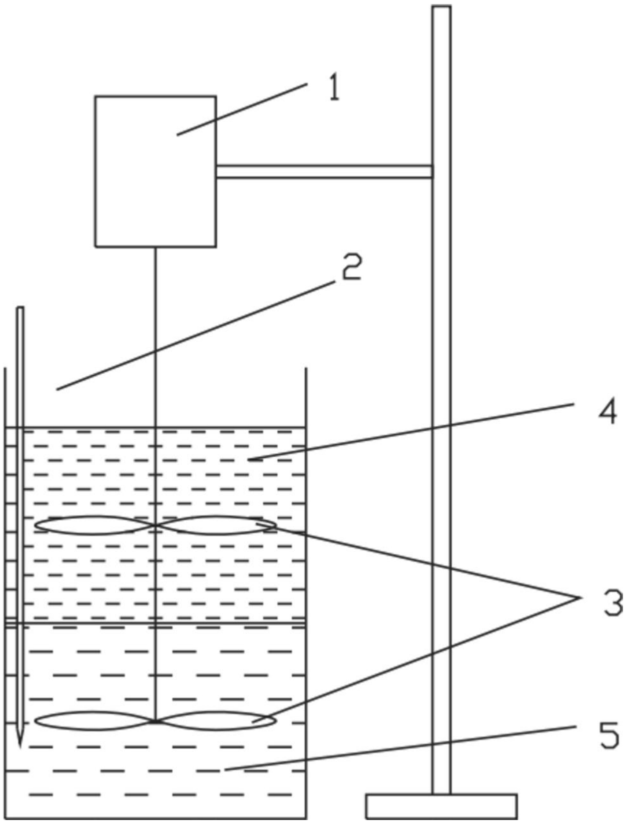

Fig. 2 A Lewis diffusion cell. 1—frequency mixing motor, 2—sampler, 3—agitating vane, 4—aqueous phase, 5—organic phase. [17]

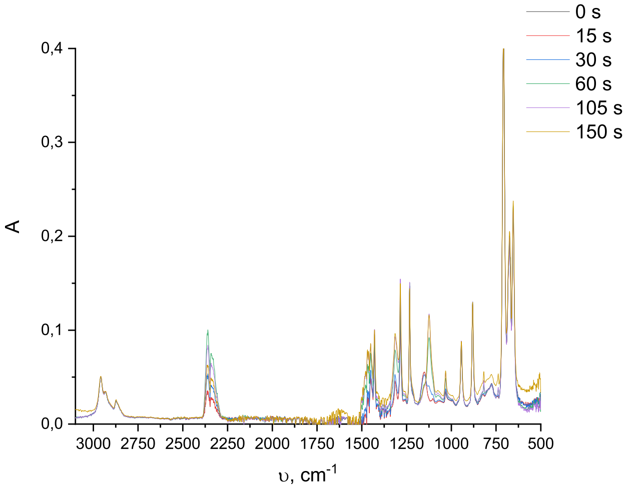

Fig. 3 IR spectra of the organic phase for europium extraction with a TAPO solution in DCE

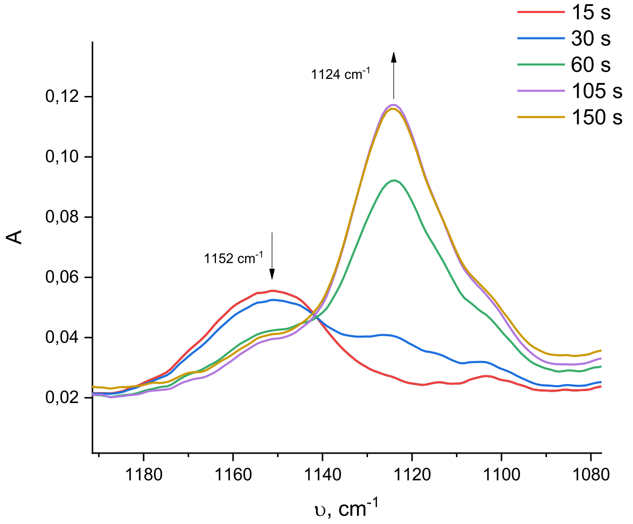

Fig. 4 IR spectra variations for the organic phase in the process of europium extraction with a TAPO solution in DCE

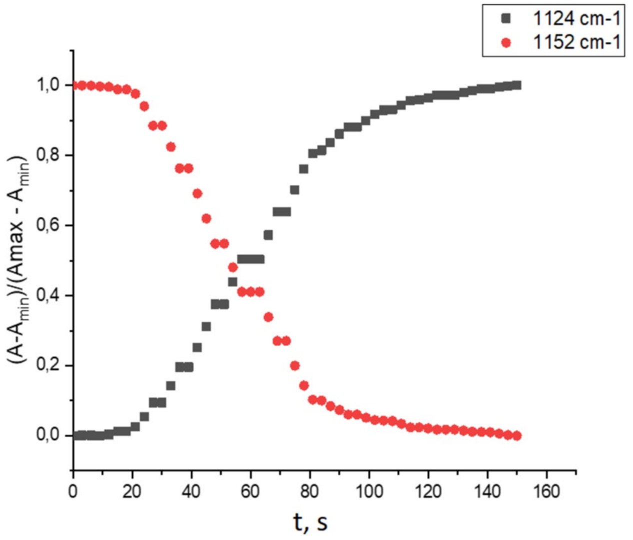

Fig. 5 Kinetic curves for europium extraction with a TAPO solution in DCE

of intact TAPO molecules at 1152 cm^{-1}, and its intensity decreases with the increasing of phase contact time. Also, with the beginning of extraction, a band of $\nu_{P=O}$ stretching vibrations of TAPO solvates with the Eu^{3+} ion at 1124 cm^{-1} appears in this region.

Taking into account the experimental data for the extraction system of europium and TAPO, we constructed kinetic curves in the coordinates $(A–A_{min})/(A_{max}–A_{min})$ *vs* t, presented in Fig. 5.

The kinetic straight lines correspond to the curves of successive reactions: up to approximately 65 s, the extraction rate increases, which can be explained by the stage of TAPO accumulation at the phase boundary due to its surface activity or by the diffusion of TAPO solvates with the Eu^{3+} ion from the surface layer to the surface of the ATR crystal. After 65 s from the moment of contact, the extraction rate can be described similarly to the rate of a first-order reversible reaction (Fig. 6) [18].

For this system, the extraction rate constant was calculated ($k = 7.5 \cdot 10^{-4}$ cm·s^{-1}), which is consistent with the literature data for a similar system of neodymium and trioctylphosphine oxide ($k = 4.8 \cdot 10^{-4}$ cm·s^{-1}) [19].

A hypothesis was proposed that the kinetic curve in Fig. 3 corresponds to two successive reactions $A \rightarrow B \rightarrow C$, where $A \rightarrow B$ is a reaction of formation of TAPO solvates with Eu^{3+} ions, and $B \rightarrow C$ is a diffusion of solvates from the surface layer to the surface of the ATR crystal. In order to study only the extraction kinetics, we minimized possible volumes of the extractant and the extracted substance. An additional experiment was conducted to study the kinetics of Eu^{3+} extraction with a TAPO solution at phase volumes of 10 µL (Fig. 7).

This kinetic curve we also reconstructed in linearizing coordinates and found the extraction kinetics constant (Fig. 8).

The calculated extraction rate constant ($k = 3.3 \cdot 10^{-4}$ cm·s^{-1}) is in better agreement with the literature data for a similar system of neodymium and trioctylphosphine oxide ($k = 4.8 \cdot 10^{-4}$ cm·s^{-1}) [19] than that with phase volumes of 50 µL. This is due to the fact that in a system with a 10 µL phase volume, the diffusion of TAPO-Eu^{3+} solvates in the lay of the organic phase to the surface of the diamond ATR makes a much smaller contribution to the kinetics, and the extraction approaches the kinetic regime. Thus, when studying the kinetics in systems with fast extraction, it is necessary to use small phase volumes. To verify the obtained results, we also investigated the kinetics by the Lewis cell method. A kinetic curve was constructed (Fig. 9) and the extraction rate constant was calculated, consistent with our data and with similar extraction rate constant ($k = 4.3 \cdot 10^{-4}$ cm·s^{-1}) (Fig. 10).

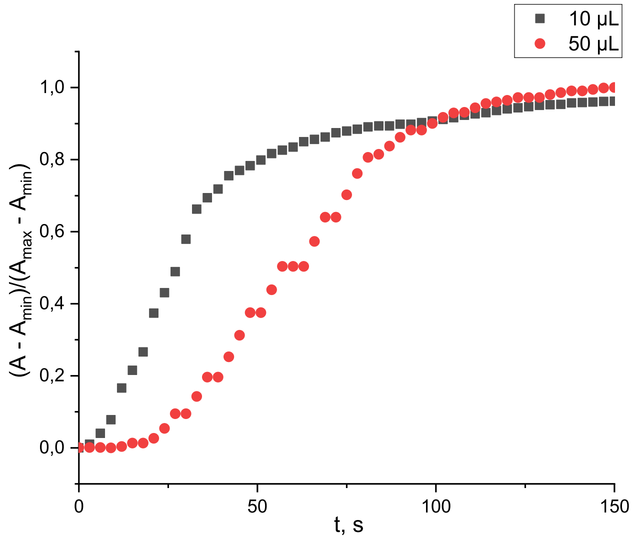

Fig. 7 Kinetic curves for europium extraction with a TAPO solution in DCE. Phase volumes are 10 µL and 50 µL, respectively

Thus, using the system of europium and TAPO, it was shown that the new ATR IR method for studying the extraction kinetics allows to carry out the experiment faster than in the Lewis cell method (the experiment time is 150 s and 1800s, respectively), while the calculated extraction rate constants are close to each other. It was also shown that the process of solvates diffusion from the surface layer to the surface of the ATR crystal has a great influence on the

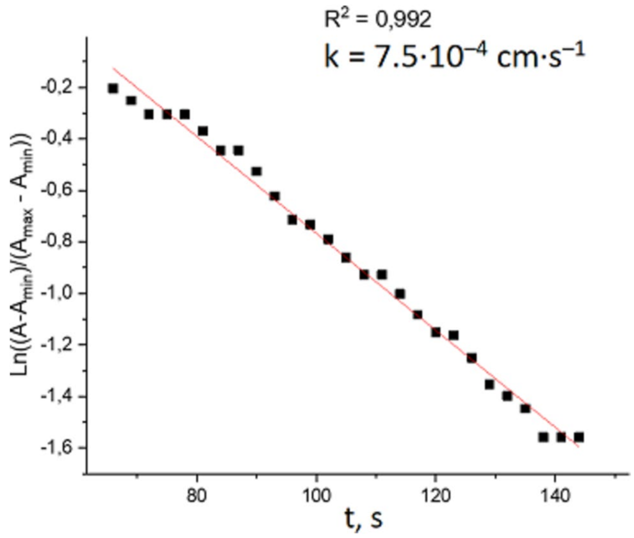

Fig. 6 The rate of europium extraction with a TAPO solution in DCE. Phase volumes are 50 µL

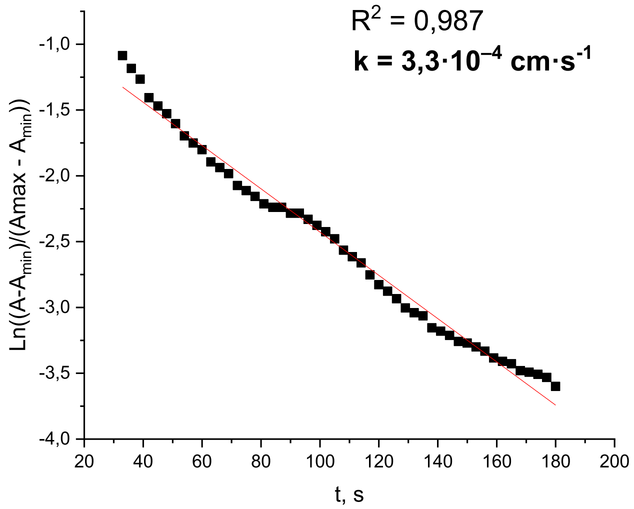

Fig. 8 Europium extraction rate with a TAPO solution in DCE. Phase volumes are 10 µL

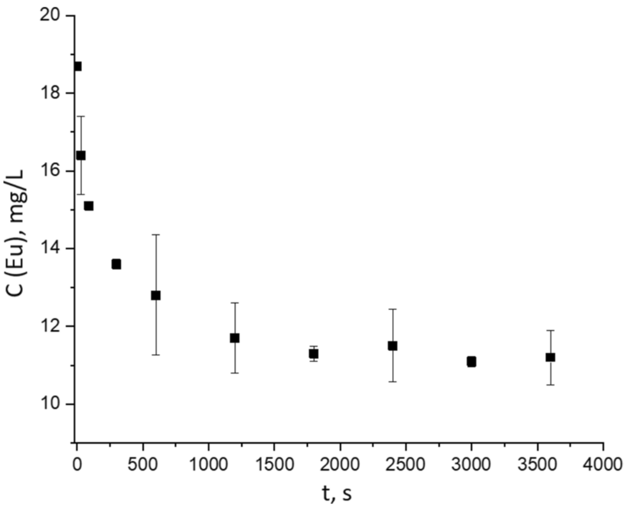

Fig. 9 Kinetic extraction curve for the system of europium and a TAPO solution in DCE, constructed for a Lewis cell

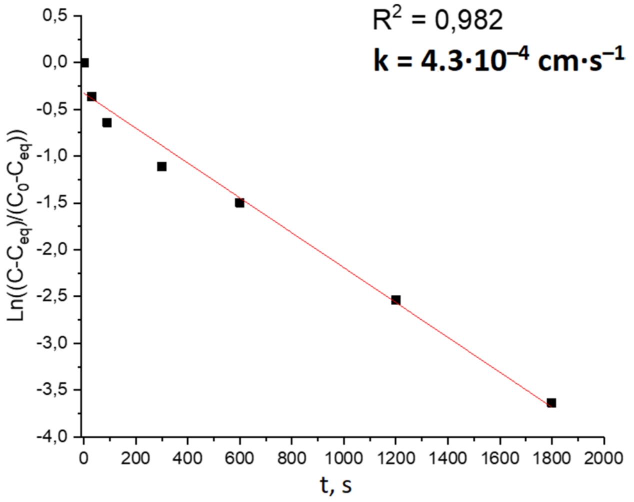

Fig. 10 Europium extraction rate for a TAPO solution in DCE, calculated for a Lewis cell

study of the kinetics, but it can be neutralized by reducing the volumes of the contacting phases.

Extraction kinetics in the system of cesium and DTBDB18C6

The study of the extraction kinetics in the system of cesium and 0.6 mol·L^{-1} DTBDB18C6 in DCE was carried out using the ATR IR method. The phase contact time was 4 h. No changes were detected in the spectra before and after extraction, so it was decided to add a salting-out agent, a substance that increases the activity of the extracted compound in the aqueous phase and also releases the extracted ions from their hydrate shell. The addition of a salting-out agent (2.5 mol·L^{-1} and 1 mol·L^{-1} HNO_3) made it possible to obtain satisfactory experimental data. Based on them, the corresponding kinetic curves were constructed (Fig. 11).

In this system the kinetic curves are not distorted by diffusion or chelate interaction. This can be explained by the long extraction process: in the system with DTBDB18C6, equilibrium is established over 90 min, while diffusion occurs much faster. This kinetic dependence also confirms the great influence of the salting-out agent on the extraction process, and is consistent with the literature data [20], showing that the optimal concentration of HNO_3 for Cs^+ extraction with DTBD18C6 is 2–3 mol·L^{-1}.

Extraction kinetics in the system of europium and CMPO

The experiments were carried out in a medium cell ($d = 4.6$ mm) with 50 µL of 0.6 mol·L^{-1} CMPO solution and 50 µL of 0.6 mol·L^{-1} $Eu(NO_3)_3$. Due to the more complex structure of the extractant, 4 $\nu_{P=O}$ stretching vibration bands were chosen for determining the kinetics of europium extraction. Thus, the region 1220–1080 cm^{-1} was regarded (Fig. 12).

This region of the spectrum contains a $\nu_{P=O}$ stretching vibration band of free CMPO molecules at 1194 cm^{-1}, with the intensity decreasing with increase of phase contact time, and a $\nu_{P=O}$ stretching vibration band at 1150 cm^{-1}, which is responsible for the vibrations of coordinated P=O groups in the solvates of the extractant with the Eu^{3+} ion.

The region of 1660–1570 cm^{-1} (Fig. 13) was also considered. It contains the band of $\nu_{C=O}$ stretching vibrations of

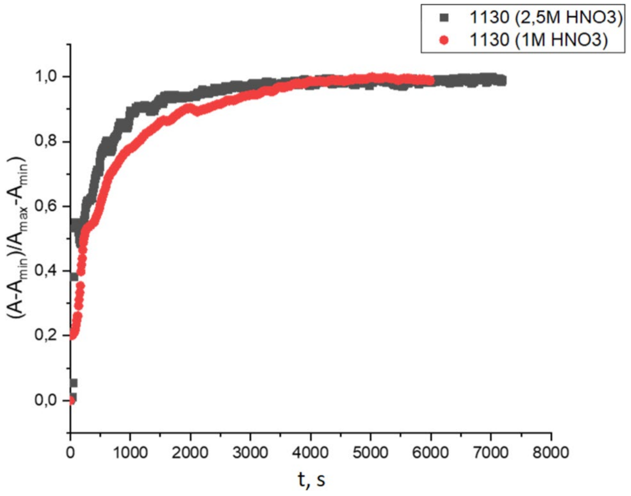

Fig. 11 Kinetic curves for cesium extraction from the aqueous phase (0.6 mol·L^{-1} $CsNO_3$ + 2.5 mol·L^{-1} HNO_3 and 0.6 mol·L^{-1} $CsNO_3$ + 1 mol·L^{-1} HNO_3) with a solution of DTBDB18C6 in DCE

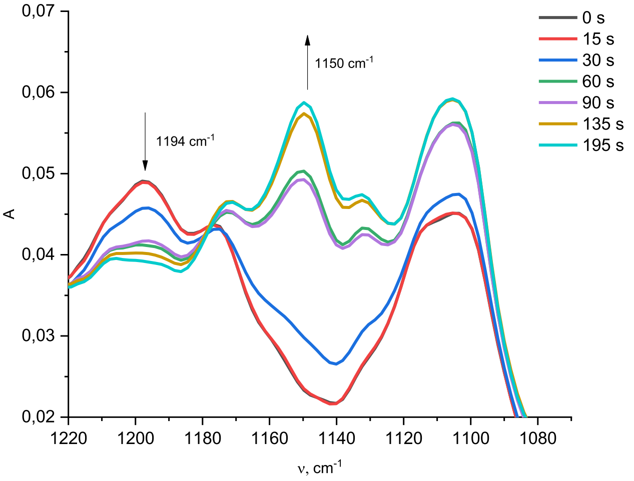

Fig. 12 IR spectra variations for the organic phase in the process of europium extraction with a CMPO solution in DCE

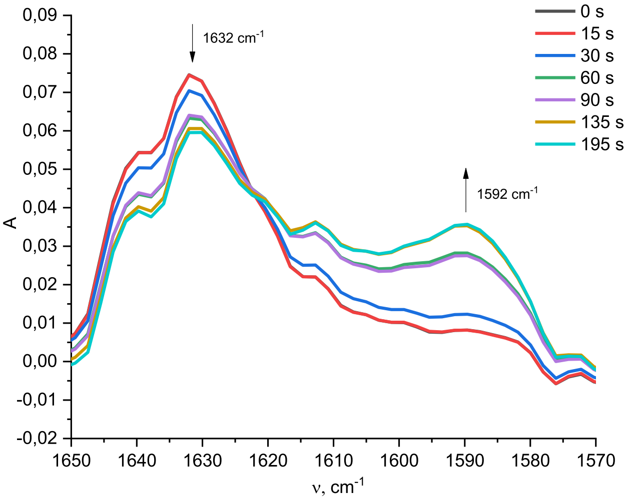

Fig. 13 IR spectra variations for the organic phase in the process of europium extraction with a CMPO solution in DCE

C=O groups uncoordinated to the metal ion at 1632 cm^{-1}, with the intensity decreasing as a result of the formation of solvates with Eu^{3+} ions, and the band of $\nu_{C=O}$ stretching vibrations at 1592 cm^{-1}, responsible for the vibrations of C=O groups of the CMPO molecule coordinated to Eu^{3+} ions.

Based on the experimental data, we constructed the kinetic curves (Fig. 14).

As it is seen from the kinetic curves, the growth of the peak responsible for the association of europium with CMPO molecules via the P=O bond is faster at the initial moment of extraction than the growth of the peak responsible for the association of europium with CMPO via the C=O bond, and then the system comes to equilibrium. The presence of two steps on the kinetic curve can be explained by the sequential addition of Eu^{3+} ions to the C=O or P=O bonds due to the chelating effect of the extractant (Fig. 15). Also, based on the fact that the peak at 1150 cm^{-1} grows faster than the peak at 1590 cm^{-1} at the initial moment of time, it can be assumed that most of the Eu^{3+} ions are primarily coordinated via the P=O bond in CMPO.

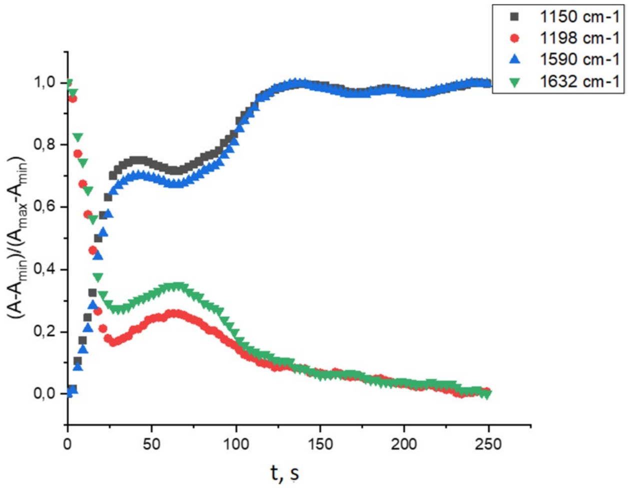

Fig. 14 Kinetic curves for europium extraction with a CMPO solution in DCE

This system was also studied by calorimetric methods. 1 mL of 0.1 mol·L^{-1} CMPO solution in DCE and 2 mL of 0.1 mol·L^{-1} aqueous Eu(NO$_3$)$_3$ solution were put into the cell of a Setaram C80 Calvet calorimeter, being separated from each other by aluminum foil. After thermal equilibrium in the system was attained, the aluminum foil was pierced with a buoy and stirring was turned on. The resulting graph of thermal effects in the system is presented at Fig. 16.

The left peak is attributed with the sample, the right one with a blank experiment without CMPO. The sharp drop at the beginning of the experiment is caused by the expansion of DCE when the buoy pierced the foil, and the subsequent exothermic effect is due to the complexation of Eu^{3+} with CMPO. It can be noted that the exo-effect of complex formation also has two steps, which confirms the theory of stepwise formation of the chelate complex. The enthalpy of complex formation when subtracting the blank experiment was – 6.1 kJ·mol^{-1}.

This experiment was also carried out on a TA Instruments Nano ITC 2G titration microcalorimeter by a CMPO solution titration with a Eu(NO$_3$)$_3$ solution. Taking into account the blank experiment, the titration curve was obtained (Fig. 17), and it also clearly shows two titration steps.

The enthalpy of complex formation in this system, calculated with the titration curve, was—24.6 kJ·mol^{-1}, which is in good agreement with literature data [21]. At the same time, the low enthalpy value in the study on a Calvet-type

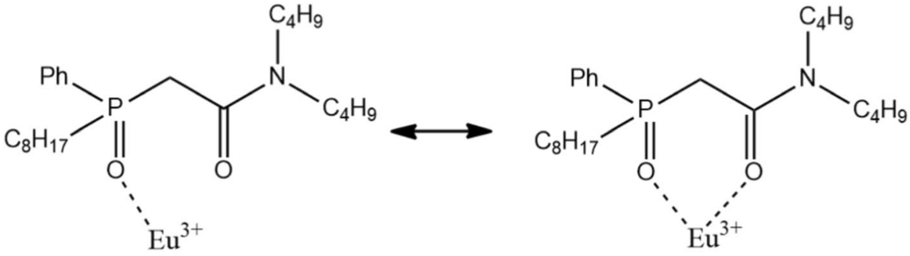

Fig. 15 Coordination and formation of the Eu^{3+} chelate complex with CMPO

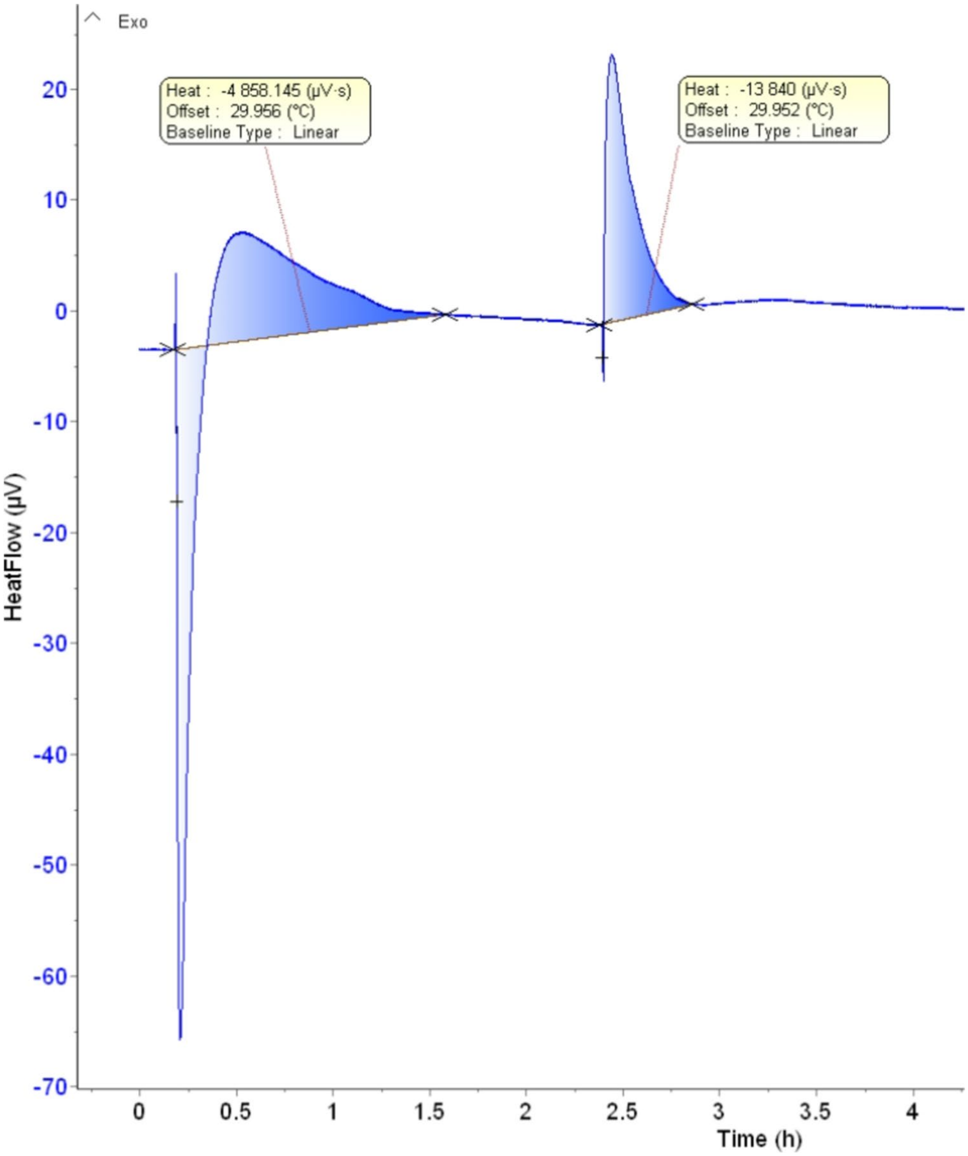

Fig. 16 Thermal effects in the system of europium and CMPO in DCE

calorimeter may be due to the weak mixing in the system, as well as the significant influence of the evaporation and expansion of DCE.

Extraction kinetics in the system of europium with TODGA

The experiments were carried out in a medium cell ($d = 4.6$ mm) with 50 µL of a 0.6 mol·L^{-1} TODGA solution in TCE and 50 µL of 0.6 mol·L^{-1} $Eu(NO_3)_3$. The spectrum region

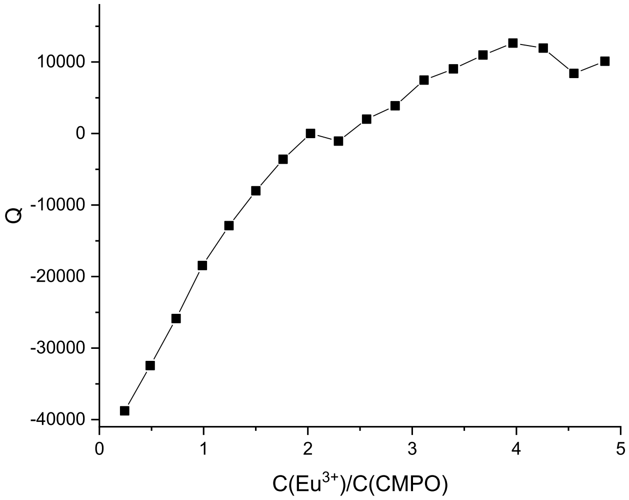

Fig. 17 Calorimetric titration curve for the system of europium and CMPO in DCE

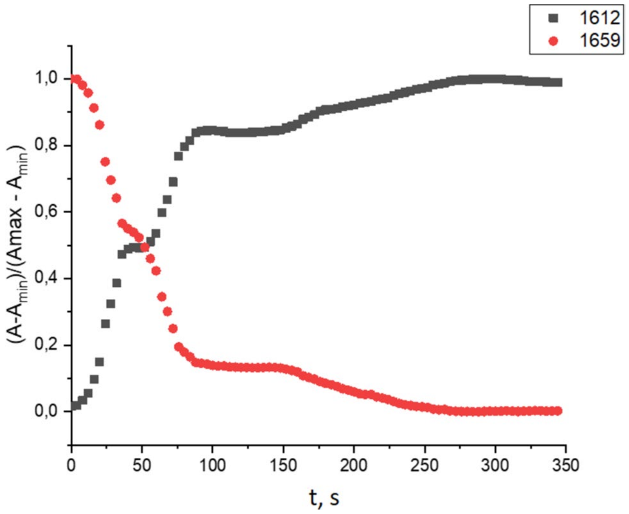

Fig. 18 Kinetic curves for europium extraction with a TODGA solution in TCE

1710–1530 cm^{-1} was analyzed. It contains a band of $\nu_{C=O}$ stretching vibrations, which is not associated with the Eu^{3+} ion of C=O groups at 1659 cm^{-1}, with the intensity decreasing during the experiment due to the formation of solvates with Eu^{3+} ions, and a band of $\nu_{C=O}$ stretching vibrations at 1612 cm^{-1}, which is responsible for the vibrations of TODGA solvates with Eu^{3+} ions. Based on the obtained experimental data, we constructed the kinetic curves in the coordinates $(A–A_{min})/(A_{max}–A_{min})$ *vs* t (Fig. 18).

Two maxima on the kinetic curves can be explained by the formation of a chelate complex (Fig. 19) and correlate with the same shape of the kinetic curves in the system with CMPO.

Thus, the above described shows that for the systems with chelate extractants, bearing functional groups of the same nature, two steps are also observed on the kinetic curve, demonstrating a chelate complex formation over the time.

Extraction kinetics for the system of yttrium and 8-HQ

Since the solubility of $Y_2(CO_3)_3$ in water is extremely low, to dissolve yttrium carbonate, a 3 mol·L^{-1} solution of K_2CO_3 was preliminarily prepared, where yttrium carbonate was then dissolved [22, 23]. A 0.01 mol·L^{-1} aqueous solution of $Y_2(CO_3)_3$ and a 0.1 mol·L^{-1} solution of 8-HQ in DCE were obtained. The spectra of 0.1 mol·L^{-1} 8-HQ solution in DCE and 8-HQ solution after extraction at 25 °C by stirring 0.5 mL of 0.01 mol·L^{-1} yttrium solution and 0.5 mL of 0.1 mol·L^{-1} 8-HQ solution were recorded, the contact time of the phases was 4 h. Since there were no visible changes in the spectra before and after extraction, it was supposed that the yttrium concentration was too low to study the kinetics in this system by the ATR IR method. This limits the new method for studying the extraction kinetics. The kinetics was studied in a Lewis cell, and a kinetic curve was constructed (Fig. 20).

Thus, on this system one can see that the ATR IR method, suggested for the extraction kinetics studying, has some limitations, for example, it can't be applied for the systems with low concentrations of the extractant and the extracted metal.

Conclusions

It is experimentally stated that the new ATR IR based method of studying the extraction kinetics allows reducing the analysis time (2–3 min instead of an hour) and significantly reducing the volume of the required aliquot of the studied solution (0.01 mL instead of tens of mL) compared to the classical methods.

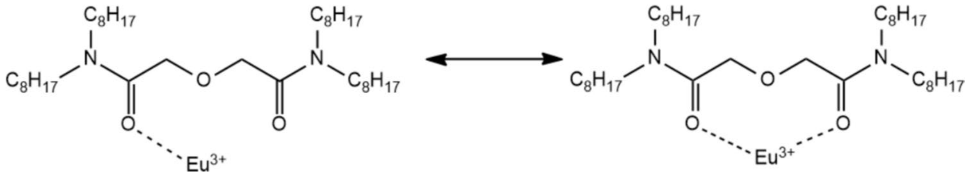

Fig. 19 Coordination and formation of the chelate complex of Eu^{3+} with TODGA

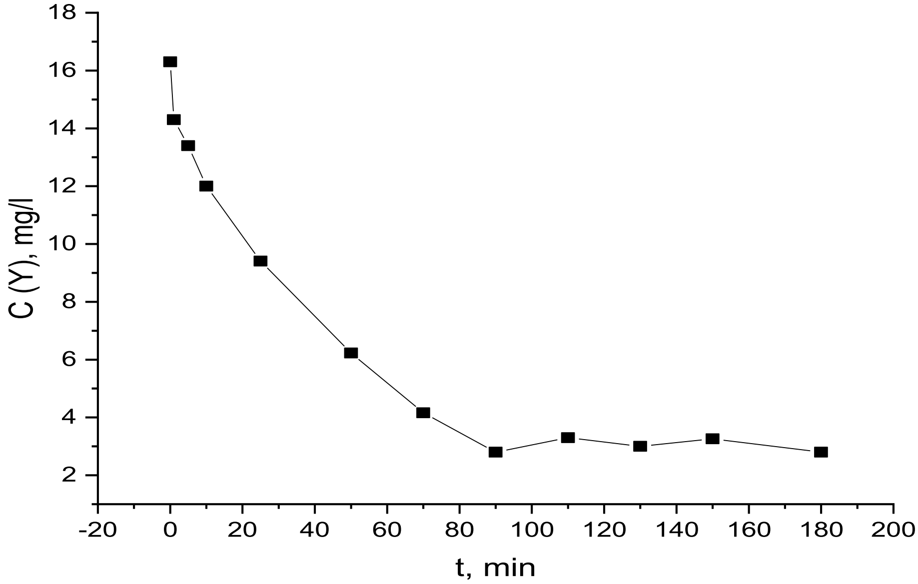

Fig. 20 Kinetic curve for yttrium extraction from 3 mol·L^{-1} K_2CO_3 with 0.1 mol·L^{-1} 8-HQ solution, obtained by the Lewis diffusion cell method

With this method some patterns of the extraction process in different extraction systems are studied. It is shown that the rate of the process can be affected both by the diffusion of the metal-extractant solvates in the extractant solution to the surface of the ATR and the mechanism of solvate formation itself. Thus, in the system of europium and CMPO the kinetic curve with two steps is explained by the stepwise formation of a chelate complex. This is confirmed by the calorimetric titration method. It is shown that for the system of europium and TAPO, the values of the extraction kinetics constants ($k_{50} = 7.5 \cdot 10^{-4}$ cm·s^{-1}, $k_{10} = 3.3 \cdot 10^{-4}$ cm·s^{-1} for the ATR IR method at different phase volumes and $k = 4.3 \cdot 10^{-4}$ cm·s^{-1} in a Lewis cell) are in good agreement with the extraction kinetics constant for a similar extraction system of neodymium and trioctylphosphine oxide ($k = 4.8 \cdot 10^{-4}$ cm·s^{-1}).

For the system of cesium and DTBDB18C6 the possibility of studying the extraction kinetics by the ATR IR method in the presence of a salting-out agent in the system is shown, and the effect of the salting-out agent (HNO_3) concentration on the distribution ratio of cesium and on the kinetics of the extraction process is stated. It is experimentally confirmed that when extracting cesium with DTBDB18C6 from aqueous solutions it is preferable to use a 2–3 mol·L^{-1} nitric acid solution. The study of the extraction kinetics in the system of yttrium and 8-HQ points out some limitations of the proposed method, namely, the potential impossibility of conducting an experiment in the case of extraction of metal cations from solutions of their poorly soluble salts. Also, for the ATR IR method, it is important for the organic phase to be denser than the aqueous one in order to contact with the ATR crystal of the attachment. The above mentioned, thus, imposes a number of restrictions on the solvents used.

Acknowledgements The work was carried out with the support of the Russian Science Foundation, project No. 24-63-00006 (https://rscf.ru/project/24-63-00006). The authors acknowledge the Resource Center "Thermogravimetric and Calorimetric Research Methods" of Saint-Petersburg State University (AAAA-A19-119082790069-6).

Data availability The authors confirm that the data supporting the findings of this study are available within the article and its supplementary materials.

Declarations

Conflict of interest All authors declare that they have no conflicts of interest.

References

1. Magnusson D, Christiansen B, Foreman MR, Geist A, Glatz JP, Malmbeck R, Sorel C (2009) Demonstration of a sanex process in centrifugal contactors using the CyMe4-BTBP molecule on a genuine fuel solution. Solvent Extr Ion Exch 27(2):97–106
2. Duan W, Zhao M, Wang C, Cao S (2014) Recent advances in the development and application of annular centrifugal contactors in the nuclear industry. Solvent Extr Ion Exch 32(1):1–26
3. Flett DS (1977) Chemical kinetics and mechanisms in solvent extraction of copper chelates. Acc Chem Res 10(3):99–104
4. Torkaman R, Safdari J, Torab-Mostaedi M, Moosavian MA (2014) A kinetic study on solvent extraction of samarium from nitrate solution with D2EHPA and Cyanex 301 by the single drop technique. Hydrometallurgy 150:123–129
5. Cao W, Huang K, Wang X, Liu H (2021) Extraction kinetics and kinetic separation of La (III), Gd (III), Ho (III) and Lu (III) from chloride medium by HEHEHP. J Rare Earths 39(10):1264–1272
6. Kasaie M, Bahmanyar H, Moosavian MA (2017) A kinetic study on solvent extraction of copper from sulfate solution with Cupromex-3302 using Lewis cell. J Environ Chem Eng 5(3):3044–3050
7. Qiang S, Zhang W, Xiong T, Xian X, Lan Z, Du Y, Fan P (2023) Extraction kinetics of lanthanum and cerium in bis (2-ethylhexyl)

phosphate (HDEHP)–lactic acid complex system using Lewis cell. Trans Nonferrous Metals Soc China 33(6):1943–1952

8. Zaitseva SV, Tyurin DV, Zdanovich SA, Koifman OI (2019) Kinetics of the Formation of an Active Oxo Species of μ-Carbidodimeric Water-Soluble Iron (IV) Sulfophthalocyanine in the Reaction with tert-Butyl Hydroperoxide. Russ J Inorg Chem 64:815–821
9. Lv H, Huang X, Feng Z, Wang M, Sun X, Peng X, Hu Y (2019) Extraction kinetics of neodymium from chloride medium using HEH/EHP saponified with magnesium bicarbonate solution. J Rare Earths 37(3):305–311
10. Jinshi D, Yang X, Liangshi W, Huang X, Zhiqi L, Shengxi W (2016) Thermodynamics and kinetics of lutetium extraction with HEH (EHP) in hydrochloric acid medium. J Rare Earths 34(3):300–307
11. Konopkina EA, Gopin AV, Pozdeev AS, Chernysheva MG, Kalle P, Pavlova EA, Matveev PI (2024) Kinetic features of solvent extraction by N, O-donor ligands of f-elements: a comparative study of diamides based on 1, 10-phenanthroline and 2, 2′-bipyridine. Phys Chem Chem Phys 26(3):2548–2559
12. Launiere CA, Gelis AV (2016) High precision droplet-based microfluidic determination of americium (III) and lanthanide (III) solvent extraction separation kinetics. Ind Eng Chem Res 55(7):2272–2276
13. Chen Z, Wang Y (2018) Solvent extraction kinetics of Sm (III), Eu (III) and Gd (III) with 2-ethylhexyl phosphoric acid-2-ethylhexyl ester. Chin J Chem Eng 26(2):317–321
14. Mojet BL, Ebbesen SD, Lefferts L (2010) Light at the interface: the potential of attenuated total reflection infrared spectroscopy for understanding heterogeneous catalysis in water. Chem Soc Rev 39(12):4643–4655
15. Baumgaertner F, Finsterwalder L (1970) On the transfer mechanism of uranium (VI) and plutonium (IV) nitrate in the system nitric acid-water/tributylphosphate-dodecane. J Phys Chem 74(1):108–112
16. Aleksandrov TS, Timoshenko VV, Brechalov AA, Smirnov IV (2023) Kinetics of the extraction of long-lived fission products present in spent nuclear fuel: a study by attenuated total reflection IR spectroscopy. Radiochemistry 65(2):226–229
17. Yang X, Wang X, Wei C, Zheng S, Sun Q, Wang D (2013) Extraction kinetics of tantalum by MIBK from pulp using Lewis cell. Hydrometallurgy 131:34–39
18. Danesi PR (2004) Solvent extraction kinetics. In: solvent extraction principles and practice, revised and expanded (pp. 218–268). CRC Press.
19. El-Hefny Naglaa E (2007) Kinetics and mechanism of extraction and stripping of neodymium using a Lewis cell. Chem Eng Process 46(7):623–629
20. Smirnov IV, Karavan MD, Kenf EV, Tkachenko LI, Timoshenko VV, Brechalov AA, Ermolenko YE (2022) Extraction of cesium, strontium, and stable simulated HLW components with substituted crown ethers in new fluorinated diluents. Solvent Extr Ion Exch 40(7):756–776
21. Hosseinnejad T, Kazemi T (2016) Complexation of amidocarbamoyl phosphine oxides with Ln+3 (Ln = La, Nd, Pm, Sm and Eu) cation series: structural and thermodynamical features. Radiochim Acta 104(2):97–105
22. De Vasconcellos ME, da ROCHA SM, Pedreira WR, Queiroz CA, Abrão A, (2006) Enrichment of yttrium from rare earth concentrate by ammonium carbonate leaching and peroxide precipitation. J Alloy Compd 418(1–2):200–203
23. Ryabukhin VA, Ryabchikov DI, Analytical chemistry of rare earth elements and yttrium, Edited by Vinogradov AP, Tananaev IV, Publication: Science, Moscow